

lncRNA SNHG6 improves placental villous cell function in an *in vitro* model of gestational diabetes mellitus

Qian Meng^{1,2}, Fang Zhang², Haixia Chen², Wen Xu², Chu Chu², Fengqing Fu^{1,3}, Fei Xia¹

¹Department of Gynecology and Obstetrics, The First Affiliated Hospital of Soochow University, Suzhou, Jiangsu, China

²Maternity Department, Lianyungang Maternal and Child Health Hospital, Lianyungang, Jiangsu, China

³Jiangsu Institute of Clinical Immunology, The First Affiliated Hospital of Soochow University, Jiangsu Key Laboratory of Clinical Immunology, Soochow University, Jiangsu Key Laboratory of Gastrointestinal tumor Immunology, Suzhou, Jiangsu, China

Submitted: 5 July 2020

Accepted: 5 September 2020

Arch Med Sci

DOI: <https://doi.org/10.5114/aoms.2020.100643>

Copyright © 2020 Termedia & Banach

Corresponding author:

Fei Xia

Department of Gynecology and Obstetrics

The First Affiliated Hospital of Soochow University

Suzhou, Jiangsu 215006

China

E-mail: xiafei0606@21cn.com

Abstract

Introduction: The purpose of this research was to investigate whether lncRNA SNHG6 has an effect on the pathogenesis of gestational diabetes mellitus (GDM).

Material and methods: Placental tissue was collected from patients with GDM and from pregnant women without GDM. Expression of lncRNA SNHG6 and EZH2 in the placental tissue was detected by qRT-PCR, immunohistochemistry (IHC), and western blotting. An *in vitro* cell model for GDM using high-dose glucose was employed to measure relative expression of mRNA and proteins by RT-qPCR and WB assay, and cell viability, apoptosis rate, invasion cell number, and wound healing rate by CCK-8, flow cytometry, transwell assay, and wound healing assay, respectively. Correlation between miRNA-26a-5p and EZH2 was investigated with a dual-luciferase reporter assay.

Results: Compared with the control placenta, lncRNA SNHG6 and EZH2 mRNA expression levels were significantly depressed and EZH2 protein expression was significantly downregulated in GDM placenta tissues ($p < 0.001$, respectively). In the *in vitro* cell model, lncRNA SNHG6 overexpression significantly improved high-dose glucose-induced HTR-8/SVneo cell function losses, including proliferation, migration, and invasion, by significantly depressing miRNA-26a-5p via regulation of EZH2 expression. The dual-luciferase reporter assay revealed that miRNA-26a-5p could target to EZH2 in HTR-8/SVneo cells.

Conclusions: Expression of lncRNA SNHG6 in the placenta of patients with GDM is abnormally decreased. Overexpression of lncRNA SNHG6 improved HTR-8/SVneo cell function via regulation of the miRNA-26a-5p/EZH2-H3K-27me3 pathway in an *in vitro* GDM model.

Key words: gestational diabetes mellitus, lncRNA, miRNA, EZH2, HTR-8/SVneo cell.

Introduction

Gestational diabetes mellitus (GDM) is a common obstetric complication with an increasing annual incidence owing to changes in maternal age, lifestyle, and diet structure [1, 2]. GDM may induce various adverse

outcomes that can pose serious hazards to maternal and fetal health, and can even have long-term impacts on both mothers and infants. It is commonly recognized that GDM has a complex pathogenesis, and this may be attributed to multiple determinants, such as inflammatory factors, insulin resistance, dysfunction of islet β -cells, genetic factors, environmental factors, and so on [3, 4]. According to previous studies, despite obvious changes in the expression of many genes with vital functions in patients with GDM, there is no obvious change in the nucleic acid sequences of these genes, and therefore these genes may be involved in the development of GDM through epigenetic mechanisms [5, 6]. Long non-coding RNA (lncRNA) expression is species and spatiotemporal specific; thus there are significant differences in the expression of lncRNA in different species and tissues, and in the same species or tissue at different time periods [7–9]. lncRNA SNHG6 is a recently discovered lncRNA that participates in tumor development by regulating expression of EZH2, the enzymatic component of polycomb repressive complex 2 (PRC2) [10–12]. EZH2 can induce trimethylation of nucleosomal histone H3 on lysine side-chain 27 (H3K27me3), and H3K27me3 can then recruit PRC2 to specific gene sites and silence expression of the target gene [13]. Cancer cell biological activities, such as invasion and migration, are similar to the biological activities of placental villous trophoblasts. However, while lncRNA SNHG2 is known to be involved in tumor development, the role of lncRNA SNHG6 remains to be clarified in GDM.

The placenta is an important location for maternal and fetal material exchange. Adhesion and invasion of trophoblasts to the endometrium contribute to placenta formation [14]. Trophoblast dysfunction may play a critical role in the development of pregnancy complications, such as pregnancy hypertension, GDM, fetal growth restriction, abortion, and so on [15, 16]. Currently, there is limited relevant information on the role of lncRNA SNHG6 and its target miRNA in trophoblasts. The present study aimed to investigate whether lncRNA SNHG6 affects the function of trophoblasts and lncRNA SNHG6's possible regulatory mechanism in GDM.

Material and methods

Subjects

Thirty pregnant women with GDM (GDM group) who were hospitalized and 30 pregnant women without GDM (control group) who were treated in our hospital between March 2018 and September 2019 were enrolled in the study. All subjects (24–28 weeks of gestation) performed a 75-g oral glucose tolerance test (OGTT). According to the standard set by the International Association of Diabetes and Pregnancy Study Group, subjects can be

diagnosed with GDM when any of the following indices exceed the threshold value: fasting blood glucose ≥ 5.1 mmol/l; blood glucose ≥ 10.0 mmol/l; or 2-hour postprandial blood glucose ≥ 8.5 mmol/l [2]. Enrolled subjects were all singleton pregnancy, without medical history of hypertension, diabetes, kidney disease, thyroid disease, infection, or cardiovascular disease. The study was approved by the Ethics Committee of our hospital.

Sampling and processing

Immediately after delivery of the placenta, small pieces of tissue (2 cm \times 2 cm \times 2 cm) were dissected from the lobule of the maternal surface of the placenta and were divided into four parts. Collected tissues were washed with phosphate-buffered saline (PBS) and either stored in 2-ml cryopreservation tubes at -80°C or fixed with 10% formaldehyde.

Paraffin-embedded section preparation and hematoxylin and eosin (HE) staining

After fixation, washing, dehydration, transparent processing, waxing, and embedding, paraffin-embedded sections were dewaxed, washed, HE stained, dehydrated and transparent processed, followed by sealing with neutral gum and observation of the stained tissues under an optical microscope (CX23, Olympus, Japan).

Immunohistochemistry (IHC)

Placental tissues ($n = 30$ for GDM and control groups) of 1 cm \times 1 cm \times 1 cm were prepared into paraffin-embedded sections according to standard procedures and were used to detect expression of EZH2 in the placenta by the immunohistochemical streptavidin-peroxidase (IHC-SP) method. Briefly, paraffin sections (4 μm thickness) were dewaxed to water, 2% boiling ethylenediaminetetraacetic acid (EDTA) solution was used for heat-induced, high-pressure antigen retrieval, then 3% H_2O_2 was applied at room temperature for 15 min to block the endogenous peroxidase, and the primary antibody was applied at 4°C overnight. All other steps strictly followed the instructions of the staining kit (Keygentec, Nanjing, China), including 3,3'-diaminobenzidine (DAB) staining, hematoxylin re-staining, and sealing. After sealing, five fields of vision (100 \times magnification) were randomly selected under an inverted phase contrast microscope for observation and photography. Under the microscope, a brownish-yellow granular precipitate was identified as positive staining. The optical density and area of development from each photograph were detected through Image-Pro Plus software, and the integrated optical density (IOD) of each specimen was calculated for semi-quantitative analysis.

Real-time PCR

Trizol extraction of total RNA was conducted from placenta samples ($n = 30$ for both GDM and control samples) and cells. ReverTra Ace qPCR RT Kit (TOYOBO, Tokyo, Japan) was utilized for reverse transcription of the cDNA of miR-26a-5p/U6, which was performed at 42°C for 60 min and at 70°C for 10 min. SYBR Green Real time PCR Master Mix (TOYOBO, Tokyo, Japan) was applied for detecting gene expression, with reaction conditions of 95°C for 10 min, followed by 40 cycles of 95°C for 10 s, 60°C for 20 s, and 72°C for 10 s. GAPDH was used as the internal reference gene (Keygentec, Nanjing, China) to detect the expression of EZH2 and lncRNA SNHG6, with amplification conditions of 95°C for 3 min, followed by 40 cycles of 95°C for 30 s, 56°C for 30 s, and 72°C for 30 s. At the end of amplification, the fusion curve was analyzed, the average *Ct* value was obtained based on data from three replicates, and the expression multiple of the target gene relative to the internal reference gene was calculated according to the formula: $2^{-\Delta\Delta Ct}$ quantitative ($\Delta Ct = Ct$ (target gene) – *Ct* (internal reference gene), $\Delta\Delta Ct =$ experimental group ΔCt – control group ΔCt). Primer sequences are shown in Table I.

Western blot (WB) assay

Radioimmunoprecipitation assay (RIPA) lysate buffer (containing 1% PMSF) was used to extract proteins from placental tissues ($n = 30$ for GDM and control samples) and cells, followed by determination of protein concentration using Coomassie Brilliant Blue. Proteins were separated by 10% SDS-PAGE according to the sampling amount of 40 μ g/well for 90 min of electrophoresis. SDS-PAGE gel extraction was conducted based on the predictive molecular weight of the target protein, followed by transfer to a polyvinylidene fluoride (PVDF) membrane using a voltage of 320 mA at 4°C. Non-specific sites were blocked with 5% bovine serum albumin (BSA) for 2 h, then the primary antibody was added for overnight incubation. After washing the membrane with TBST for 15 min, the secondary

antibody was added with incubation at room temperature for 1 h. The membrane was then washed three times with TBST, the ECL method was used for development and exposure, and the gray value was scanned and recorded using Image J software (National Institutes of Health, Bethesda, MD, USA). The gray value ratio of the target protein and the internal reference protein was analyzed as the relative expression of the target protein.

Cell culture

Human chorionic trophoblast cells (HTR-8/SVneo cells; ATCC, USA) were cultured at 37°C and 5% CO₂ in Dulbecco's Modified Eagle Medium (DMEM) containing 10% fetal bovine serum (FBS) and 1% penicillin and streptomycin double-antibiotic solution. Except for the normal control (NC) group, all cells in other groups were treated with 30 mmol/l glucose.

Experimental groups were as follows: NC group, HTR-8/SVneo cells treated with low dose of glucose; Model group, HTR-8/SVneo cells treated with high dose of glucose; lncRNA group, HTR-8/SVneo cells transfected with lncRNA SNHG6 and treated with high-dose glucose; miR-inhibitor group, HTR-8/SVneo cells transfected with miR-26a-5p inhibitor and treated with high-dose glucose; lncRNA + miRNA group, HTR-8/SVneo cells transfected with miR-26a-5p and lncRNA SNHG6 and treated with high-dose glucose.

Cell transfection

On the day before transfection, actively growing cells were seeded in 6-well plates at a concentration of 3×10^5 cells/well, and transfection was performed when the cell density reached 50–60%. The nanocomposite formed by P5RHH-loaded miRNA, miR-inhibitor, and lncRNA SNHG6, respectively, was used for corresponding transfection, including lncRNA, miR-inhibitor, and lncRNA + miRNA groups (co-transfection of miRNA-26a-5p and lncRNA SNHG6). Subsequent experiments were conducted 24 h after transfection and after 48 h of high-dose glucose culture.

Table I. List of RT-PCR primers

Gene name	Forward primer (5'-3')	Reverse primer (5'-3')
SNHG6	TTGAGGTGAAGGTGTATG	GGTAACGAAGCAGAAGTA
miR-26a-5p	CGTCTTCAAGTAATCCAGGA	GCAGGGTCCGAGGTATTC
EZH2	CGAGCTCCTCTGAAGCAAAT	AACCTAGCAATGGCACAGAAA
GAPDH	GGATTTGGTGTGCTATTGGGC	CGCTCTGGAAGATGGTGAT
U6	TGCGGGTGCTCGCTTCGACGC	CCAGTGCAGGGTCCGAGGT

CCK-8 colorimetry for cell proliferation

After continuous culture for 48 h, cells were seeded in 96-well plates at a concentration of 3×10^5 cells/well and incubated for a further 48 h at 37°C and 5% CO₂. Ten microliters of CCK-8 reagent were then added to each well with mixing, and plates were incubated for 1 h in the dark. A microplate reader was used to measure the absorbance of the wells at a wavelength of 450 nm to calculate the cell activity of each experimental group. Six replicates were set for each group.

Flow cytometry for cell apoptosis

After 48 h of corresponding treatment for cells in each group, the culture supernatant was discarded and cells were washed twice with cool PBS, followed by digestion with 0.25% trypsin. Cells were collected by centrifugation at 800 rpm for 5 min, then resuspended in 100 µl 1× binding buffer. With the addition of 5 µl of Annexin-V APC and 5 µl 7-AAD separately, the cell suspension was mixed well and incubated at room temperature in the dark for 30 min. The cells were analyzed by Well Biotechnology, Co., Ltd. (China) using Cytomics FC500 (Beckman Coulter, Brea, CA, USA).

Transwell assay

With corresponding cell treatment for 48 h in each group, cells were digested with trypsin, resuspended in serum-free medium, and the cell density was adjusted to 4×10^4 cells/l. One hundred microliters of cell suspension was added to the upper layer of a Transwell chamber, and 500 µl of DMEM containing 10% FBS was added to the lower layer. Following further culture in a 5% CO₂ incubator at 37°C for 24 h, the chamber was removed and washed three times with PBS. After wiping non-migrated cells from the upper chamber using wet cotton swabs, cells were fixed with 4% paraformaldehyde for 20 min, and then stained with 0.1% crystal violet for 10 min. The membrane was slightly cut using the blade at the bottom of the chamber, followed by sealing with resin. Under an inverted phase contrast microscope (200× magnification), five fields of vision were randomly selected to count the number of cells passing through the membrane.

Wound healing assay

Cells in each group were treated accordingly, then a 10-µl pipette head was used to slightly scratch along a straight line at the central axis of the culture plate. After removal of the floating cells by rinsing with PBS, plates were incubated for a further 24 and 48 h. The distance between scratches at 0, 24, and 48 h was then observed un-

der an optical microscope (CX23, Olympus, Japan), and the migration ability of cells in each group was expressed by the percentage of cell scratch healing. Wound healing rate (%) = (0 h width – 24 h or 48 h width)/0 h width × 100.

Dual-luciferase reporter assay

A dual-luciferase reporter assay was performed with the construction of luciferase reporter gene plasmids containing potential binding sites in the 3'-untranslated region (UTR) of the EZH2 gene, including the wild-type EZH2 gene 3'-UTR and mutant EZH2 gene 3'-UTR. Plasmids were stored at –20°C. Plasmids containing miR-26a-5p were then co-transfected into HTR-8/SVneo cells and cultured for 48 h, and luciferase activity was measured using a commercially available kit (Keygentec, Nanjing, China).

Statistical analysis

SPSS22.0 software (Armonk, IL, USA) was used for statistical analysis in this study. The results are expressed as mean ± SD. Comparisons of the four diet groups were performed by one-way analysis of variance (ANOVA), and post hoc analyses were used with Tukey's test for multiple comparisons. *P*-values of less than 0.05 for ANOVA and post hoc analyses were used for assessment.

Results

HE staining of placental tissue

In placental tissue samples from the control group, villi were uniform in size, and regular in distribution and morphology. There was a monolayer distribution of villous trophoblasts, and syncytiotrophoblasts and cytotrophoblasts were rare (Figure 1 A). Placental tissue from the GDM group had mature and immature areas of terminal villi. Villous trophoblasts were monolayer distributed, with an obvious increase in syncytiotrophoblasts and cytotrophoblasts compared with the control group (Figure 1 A).

Expression levels of SNHG6 and related genes and proteins in placental tissue

RT-PCR showed significantly decreased expression of lncRNA SNHG6 and EZH2 in placental tissue from the GDM group compared with that of the control group (*p* < 0.001, respectively, Figure 1 B). IHC and WB indicated that EZH2 protein was expressed in the placental tissue from both groups of pregnant women (Figures 1 C, D). However, expression of EZH2 protein in the trophoblasts of the GDM group was significantly lower than in the control group, and this difference was statistically significant (*p* < 0.001, respectively, Figures 1 C, D).

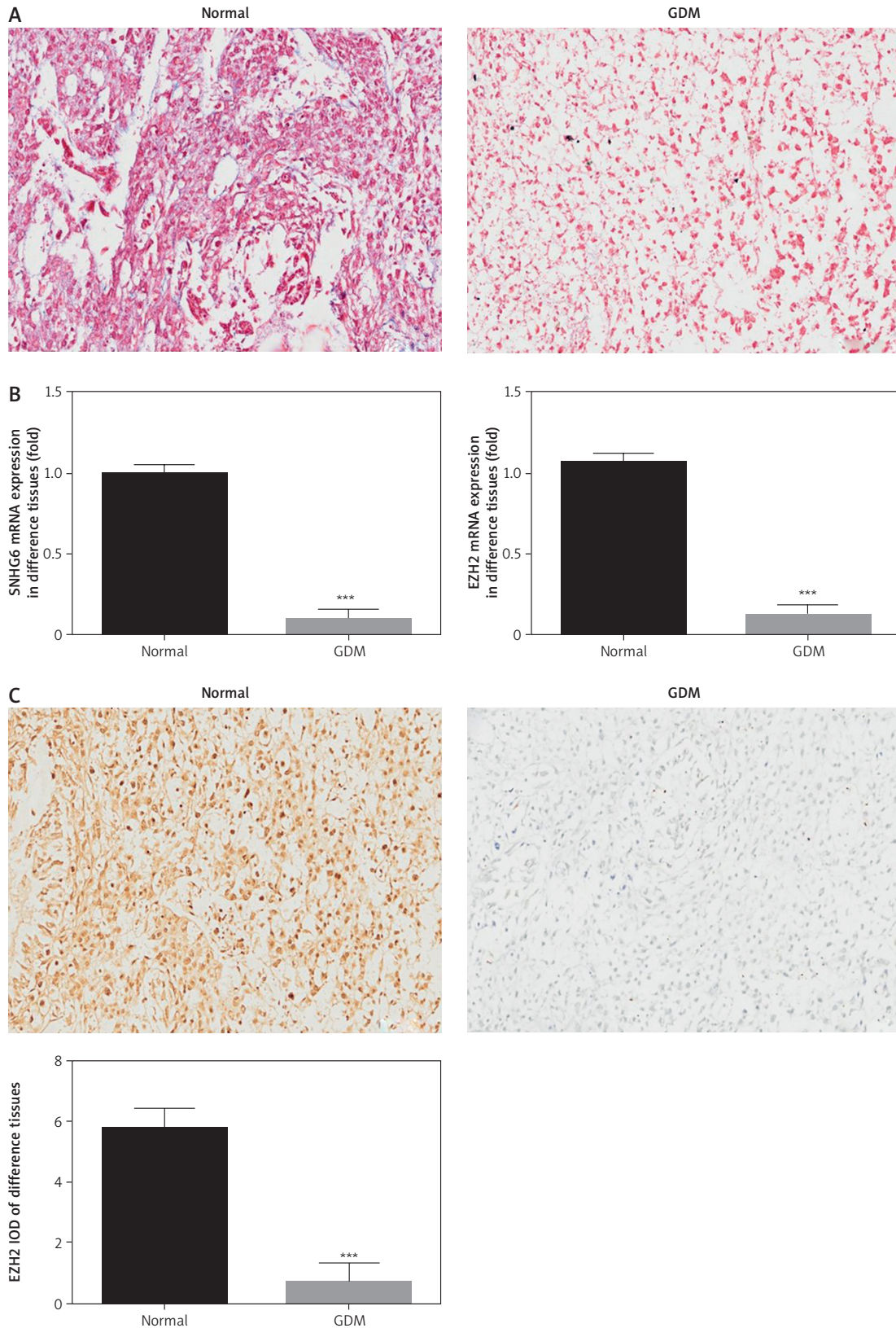


Figure 1. Placental pathology and expression of lncRNA SNHG6 and EZH2 in placental tissues from subjects with and without GDM. **A** – Placental pathology by HE staining (100× magnification). **B** – Relative mRNA expression by RT-PCR. EZH2 protein expression by IHC (×100 magnification) (**C**) and WB (**D**)

Control – placenta from subject without GDM, GDM – placenta from subject with GDM. *** $P < 0.001$, compared with control.

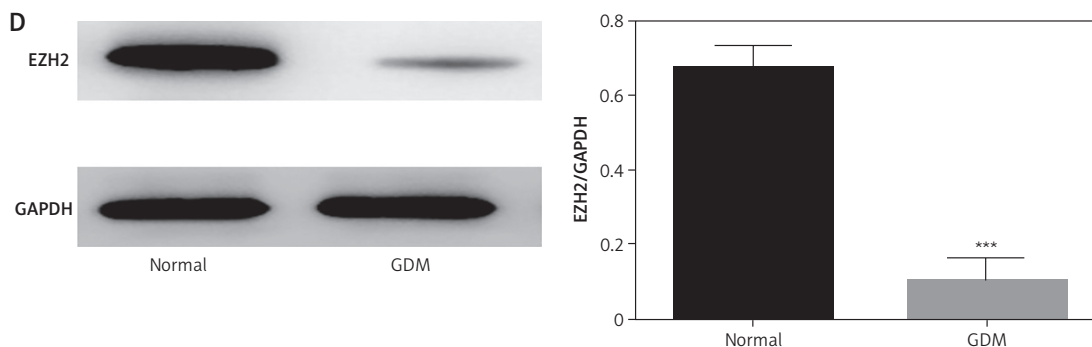


Figure 1. Cont. **B** – Relative mRNA expression by RT-PCR. EZH2 protein expression by IHC ($\times 100$ magnification) (**C**) and WB (**D**)

Control – placenta from subject without GDM, GDM – placenta from subject with GDM. *** $P < 0.001$, compared with control.

In vitro effects of SNHG6 on expression of related genes and on cell proliferation and apoptosis

In the *in vitro* GDM model, RT-PCR showed that the Model group had an obvious decrease in mRNA expression of SNHG6 and EZH2 compared with the NC group ($p < 0.001$, Figures 2 A, B), but there was a significant increase in expression of miR-26a-5p mRNA ($p < 0.001$, Figure 2 C). Compared with the Model group, the lncRNA group had a significant increase in mRNA expression of SNHG6 and EZH2 ($p < 0.001$, respectively, Figures 2 A, B), but an evident decrease in miR-26a-5p mRNA expression ($p < 0.001$, Figure 2 C). Furthermore, CCK-8 assays and flow cytometry analysis revealed that cell proliferation in the Model group was significantly decreased and the apoptotic rate was significantly increased compared with cells of the NC group ($p < 0.001$, Figures 2 D, E). Following transfection of lncRNA SNHG6 into cells, proliferation activity significantly increased while the apoptotic rate significantly decreased compared with cells of the Model group ($p < 0.001$, Figures 2 D, E).

Effect of SNHG6 on cell invasion and migration *in vitro*

Compared with the NC group, the number of invasive cells in the Model group was significantly reduced, and the wound healing rate of Model group cells was inhibited at 24 and 48 h ($p < 0.001$, Figures 3 A, B). Transfection of lncRNA SNHG6 into cells (lncRNA group) resulted in a significantly higher number of invasive cells than in the Model group, and a significant increase in the wound healing rate of cells at 24 and 48 h ($p < 0.001$, Figures 3 A, B).

In vitro effect of SNHG6 on expression of related proteins

WB revealed decreased expression of EZH2 and H3K27me3 proteins in the Model group compared

with the NC group ($p < 0.001$, Figure 4). Transfection of lncRNA SNHG6 into cells (lncRNA group) resulted in significantly increased expression of EZH2 and H3K27me3 proteins compared with that of the Model group ($p < 0.001$, respectively, Figure 4).

Gene expression, cell proliferation, and apoptosis in each *in vitro* experimental group

RT-PCR was used to analyze gene expression of lncRNA SNHG6, EZH2, and miRNA-26a-5p. Compared with the NC group, the Model group and miR-inhibitor group had evidently decreased expression of lncRNA SNHG6 ($p < 0.001$, respectively, Figure 5 A). The Model group also showed decreased gene expression of EZH2 ($p < 0.001$, Figure 5 B), and significantly increased gene expression of miR-26a-5p ($p < 0.001$, Figure 5 C). Furthermore, compared with the Model group, the lncRNA + miRNA group had significantly increased gene expression of lncRNA SNHG6 ($p < 0.001$, Figure 5 A), and the miR-inhibitor group exhibited much higher gene expression of EZH2 but obviously lower gene expression of miR-26a-5p ($p < 0.001$, respectively, Figures 5 B, C). Co-transfection of lncRNA SNHG6 and miRNA-26a-5p into cells (lncRNA + miRNA group) resulted in a significant decrease in gene expression of EZH2 and an obvious increase in expression of miR-26a-5p compared with that in the miR-inhibitor group ($p < 0.001$, Figures 5 B, C).

Using the CCK-8 assay, the Model group exhibited a decrease in cell proliferation activity compared with that of the NC group (Figure 5 D). When the miR-26a-5p inhibitor was transfected into cells (miR-inhibitor group), there was an increase in cell proliferation compared with that of the Model group (Figure 5 D). Co-transfection of lncRNA SNHG6 and miRNA-26a-5p into cells (lncRNA + miRNA group) resulted in significantly lower cell proliferation activity than that observed

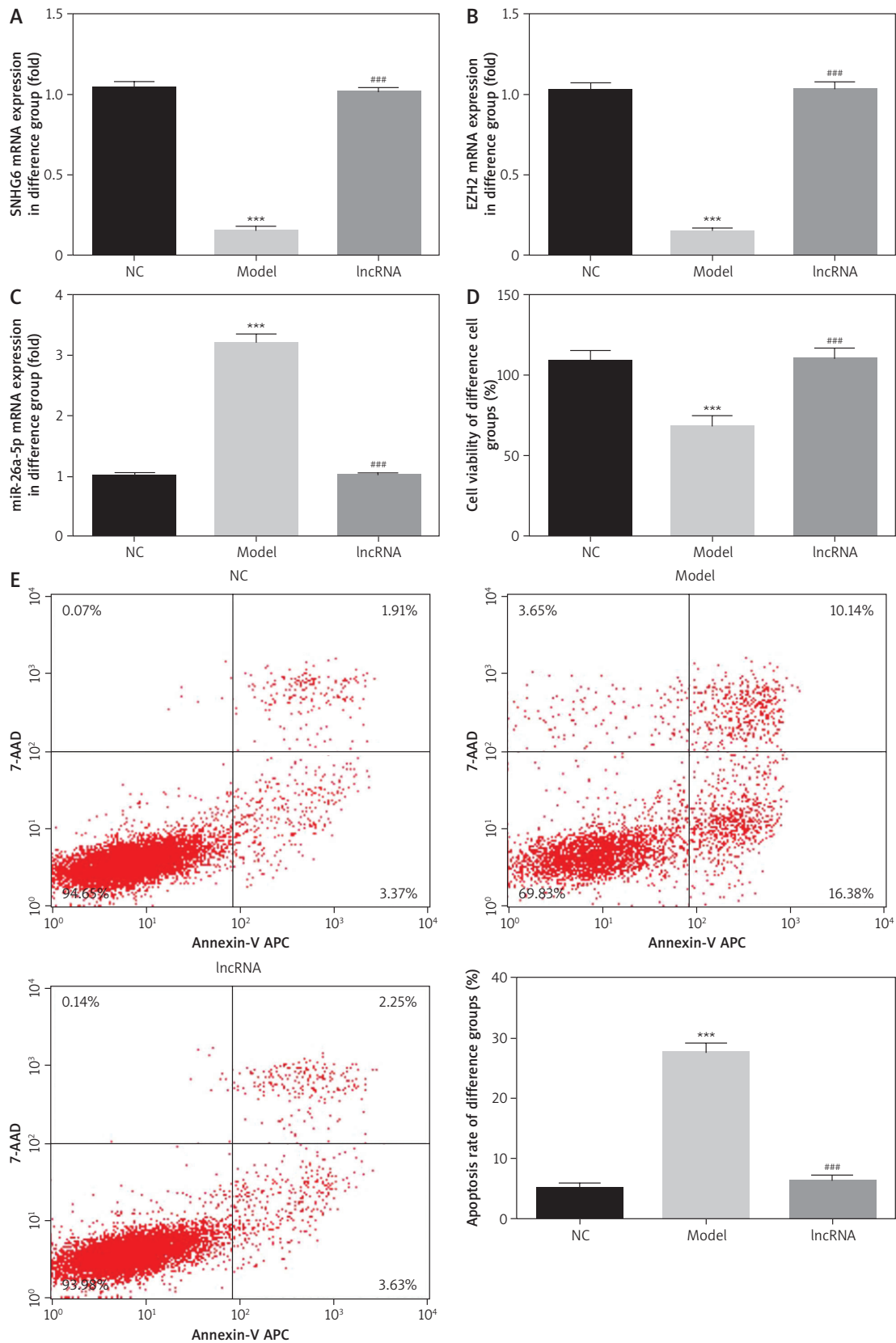


Figure 2. Relative mRNA expression, cell proliferation, and apoptosis rate of different experimental groups in an *in vitro* cell model of GDM. **A** – SNHG6 mRNA expression by RT-PCR assay. **B** – EZH2 mRNA expression by RT-PCR assay. **C** – miR-26a-5p mRNA expression by RT-PCR assay. **D** – Cell viability by CCK-8 assay. **E** – Apoptosis rate. NC – normal control group, Model – cells treated with high-dose glucose, lncRNA – cells transfected with lncRNA SNHG6 and treated with high-dose glucose. ****P* < 0.001, compared with NC group; ###*p* < 0.001, compared with Model group.

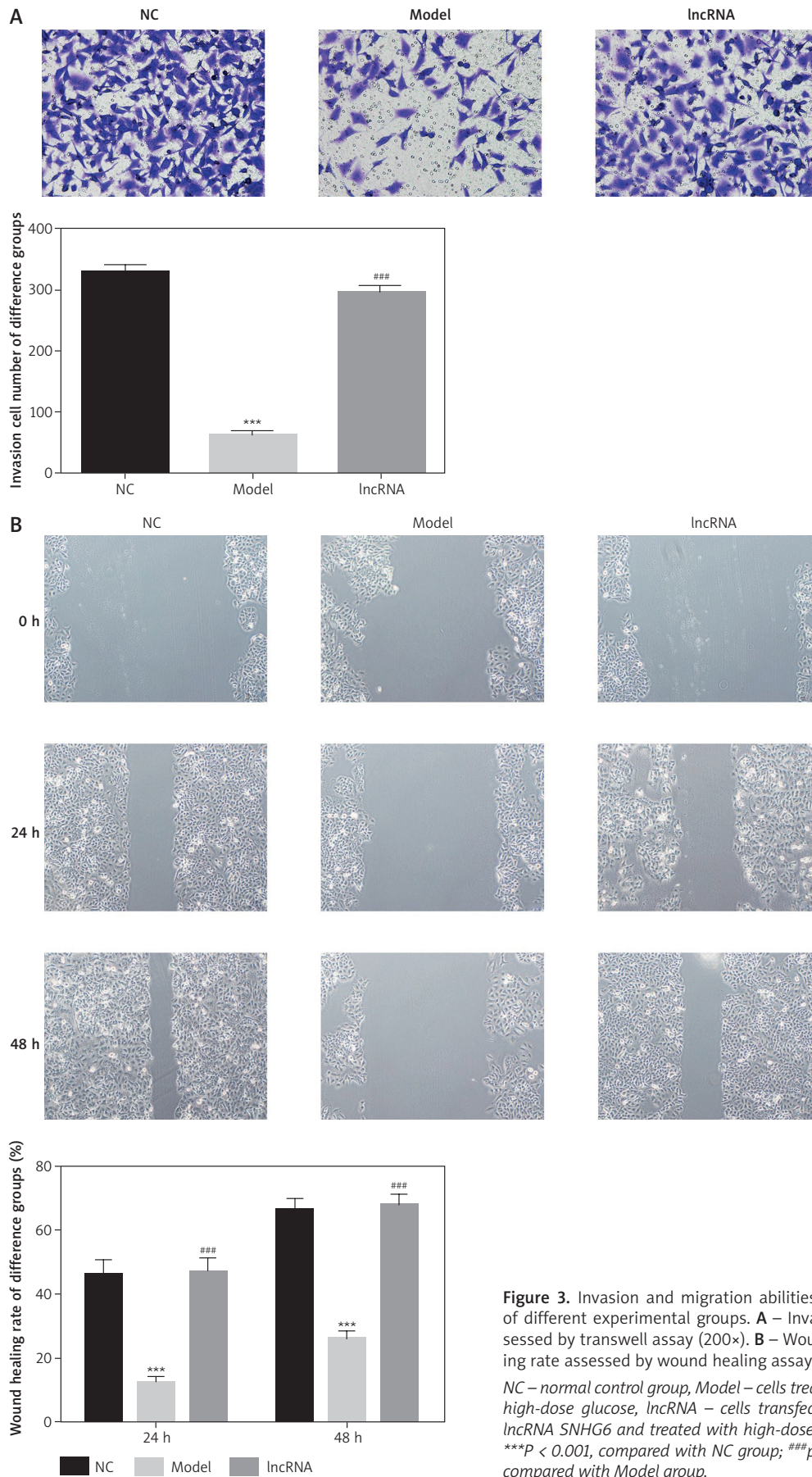


Figure 3. Invasion and migration abilities of cells of different experimental groups. **A** – Invasion assessed by transwell assay (200×). **B** – Wound healing rate assessed by wound healing assay (100×). NC – normal control group, Model – cells treated with high-dose glucose, lncRNA – cells transfected with lncRNA SNHG6 and treated with high-dose glucose. *** $P < 0.001$, compared with NC group; ### $p < 0.001$, compared with Model group.

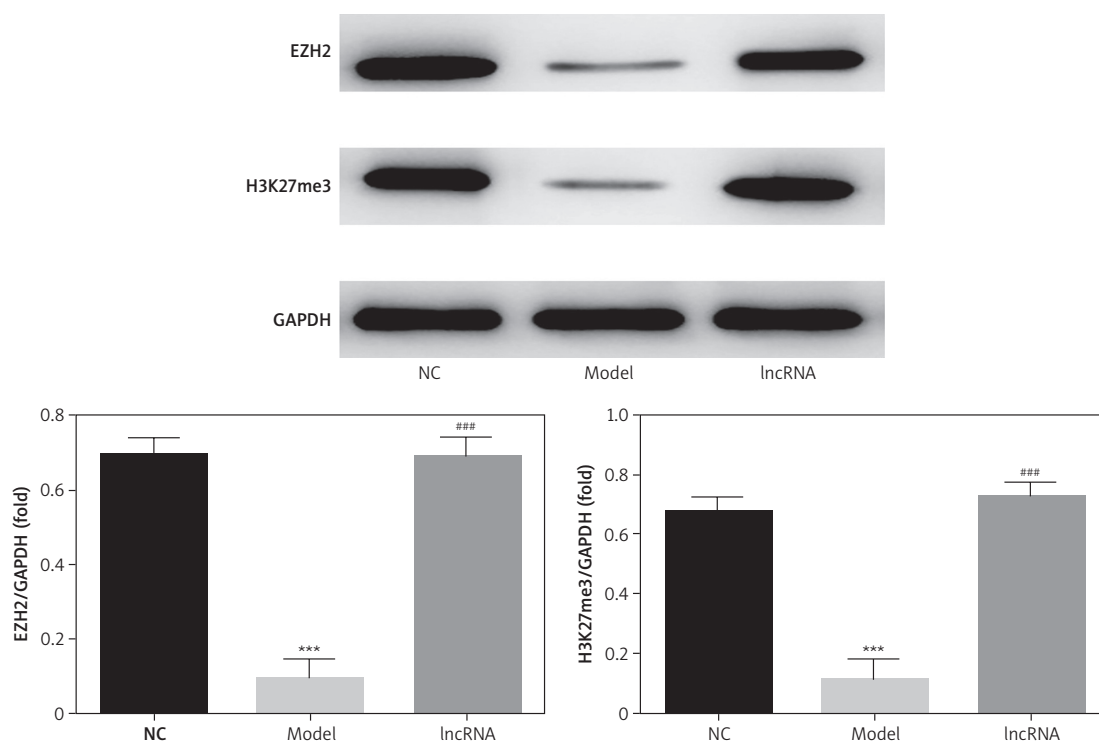


Figure 4. Relative protein expression, determined by WB, of different experimental groups in an *in vitro* cell model of GDM

NC – normal control group, Model – cells treated with high-dose glucose, lncRNA – cells transfected with lncRNA SNHG6 and treated with high-dose glucose. *** $P < 0.001$, compared with NC group, ### $P < 0.001$, compared with Model group.

in the miR-inhibitor group ($p < 0.001$, Figure 5 D). Meanwhile, flow cytometry analysis demonstrated an obvious decrease in the apoptosis rate in the Model group compared with that of the NC group, while the apoptosis rate was significantly increased in the miR-inhibitor group compared with that of the Model group (Figure 5 E). Co-transfection of lncRNA SNHG6 and miRNA-26a-5p into cells (lncRNA + miRNA group) resulted in an obvious decrease in apoptosis rate when compared with the miR-inhibitor group ($p < 0.001$, Figure 5 E).

Cell invasion and migration abilities in each *in vitro* experimental group

Transwell assays were used to investigate cell invasion in the different experimental groups. Compared with the NC group, the Model group had significantly fewer invasive cells, while the number of invasive cells in the miR-inhibitor group was obviously upregulated compared with the Model group (Figure 6 A). Co-transfection of lncRNA SNHG6 and miRNA-26a-5p into cells (lncRNA + miRNA group) resulted in a decrease in the number of invasive cells when compared with the miR-inhibitor group ($p < 0.001$, Figure 6 A). The wound healing assay revealed that the rate of wound healing was sig-

nificantly decreased at 24 and 48 h in the Model group compared with that of the NC group. Transfection of the miR-26a-5p inhibitor into cells (miR-inhibitor group) resulted in an obvious increase in wound healing rate at both time points compared with the rates in the Model group. Following co-transfection of lncRNA SNHG6 and miRNA-26a-5p into cells (lncRNA + miRNA group), there was a significant decrease in the wound healing rate at 24 and 48 h compared with that of the miR-inhibitor group ($p < 0.001$, Figure 6 B).

WB detection of related protein expression in each *in vitro* experimental group

WB revealed obvious downregulation in expression levels of EZH2 and H3K27me3 proteins in the Model group when compared with those in the NC group. Transfection of miR-26a-5p inhibitor (miR-inhibitor group) resulted in an increase in protein expression of EZH2 and H3K27me3 when compared with expression levels in the Model group. Cells co-transfected with lncRNA SNHG6 and miRNA-26a-5p (lncRNA + miRNA group) exhibited significant decreases in EZH2 and H3K27me3 protein expression when compared with levels in the miR-inhibitor group ($p < 0.001$, respectively, Figure 7).

Correlation analysis of miR-26a-5p and EZH2

The dual-luciferase reporter assay demonstrated that there was no significant difference in luciferase activity between the miR-NC group and the miR-26a-5p group in EZH2-Mul cells. However, in EZH2-WT cells, the miR-26a-5p group had significantly reduced luciferase activity compared with that of the miR-NC group ($p < 0.001$, Figure 8).

Discussion

GDM is a common disease in pregnancy, and one of the risk factors of adverse events in pregnant women and fetuses. There has been increased focus on epigenetic studies of GDM and lncRNA in recent decades. lncRNA H19 was the first lncRNA reported to be associated with GDM, and may cause insulin secretion restriction by affecting the function of islet cells [10]. Abnormal expression of lncRNAs is reported to be intimately associated with the occurrence of GDM and can affect the status of placental cells during pregnancy [11, 12]. In our study, expression of lncRNA SNHG6 in the placenta of patients with

GDM was abnormally low, suggesting that lncRNA SNHG6 may be involved in the pathogenesis of GDM. Furthermore, in an *in vitro* model of GDM, transfection of lncRNA SNHG6 into HTR-8/SVneo cells resulted in effective inhibition of the damaging activity (proliferation, invasion and migration) caused by high-dose glucose stimulation. Simultaneously, expression of miR-26a-5p decreased significantly with the increase in lncRNA SNHG6 expression. It was thus speculated that lncRNA SNHG6 might act through miR-26a-5p.

MicroRNAs (miRNAs) are a class of highly conserved, small non-coding RNAs that have unique functions at the post-transcriptional level (epigenetics). Studies have shown that miRNAs are closely related to many important physiological and pathological processes *in vivo* and play a “dynamic regulator” role in cell function and metabolic regulation [17]. Correlation between miRNAs and GDM is a relatively new area of research and, to date, there are only limited studies with small sample sizes reporting on this correlation [18, 19]. However, there are some *in vitro* and simulation experiments that provide theoretical support for

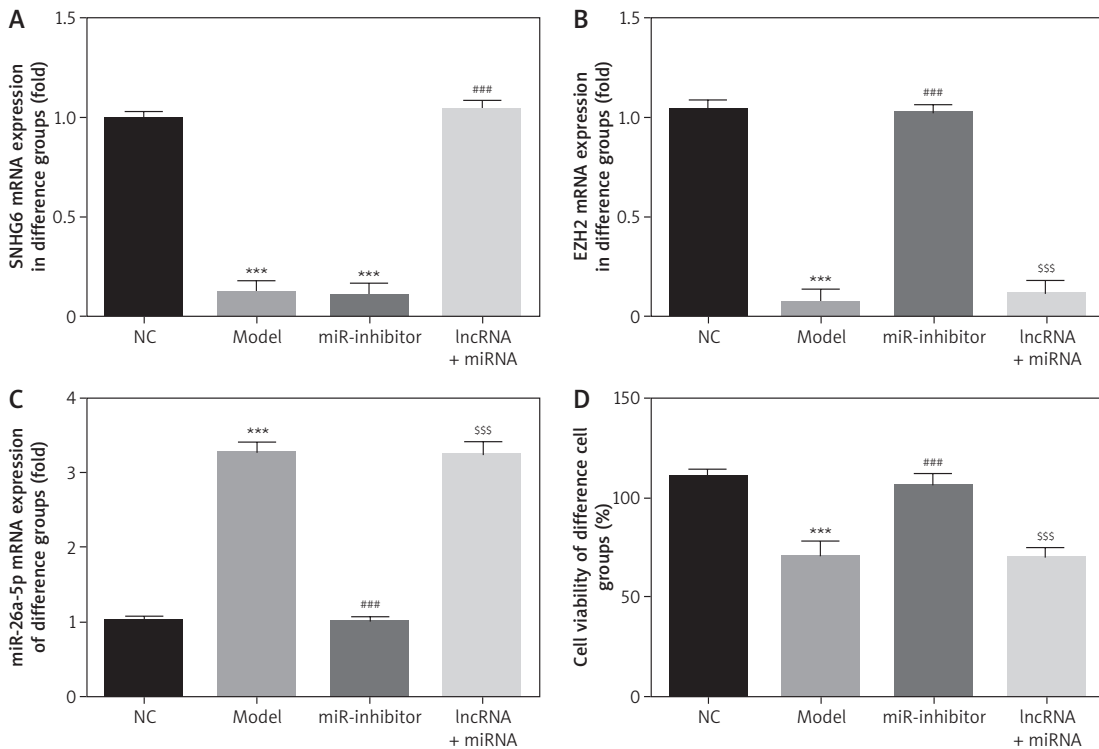


Figure 5. Effects of miRNA-26a-5p on relative mRNA expression, cell proliferation, and apoptosis rate of different experimental groups in an *in vitro* cell model of GDM. **A** – SNHG6 mRNA expression by RT-PCR assay. **B** – EZH2 mRNA expression by RT-PCR assay. **C** – miRNA-26a-5p mRNA expression by RT-PCR assay. **D** – Cell viability determined by CCK-8 assay

NC – normal control group, Model – cells treated with high-dose glucose; miR-inhibitor: cells transfected with miRNA-26a-5p inhibitor and treated with high-dose glucose, lncRNA + miRNA: cells transfected with lncRNA SNHG6 and miRNA-26a-5p and treated with high-dose glucose. *** $P < 0.001$, compared with NC group, ### $p < 0.001$, compared with Model group, ^{SSS} $p < 0.001$, compared with miR-inhibitor group.

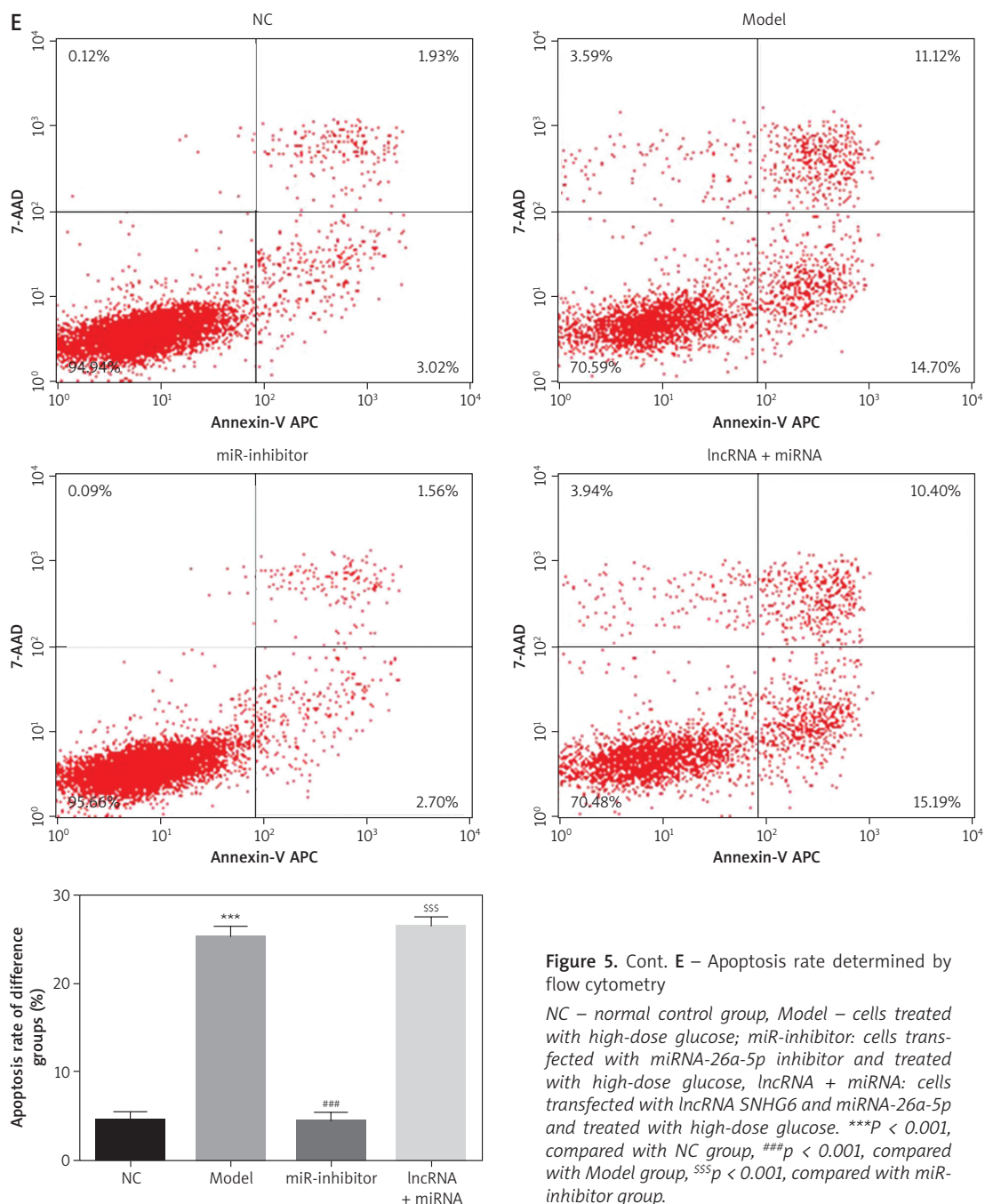
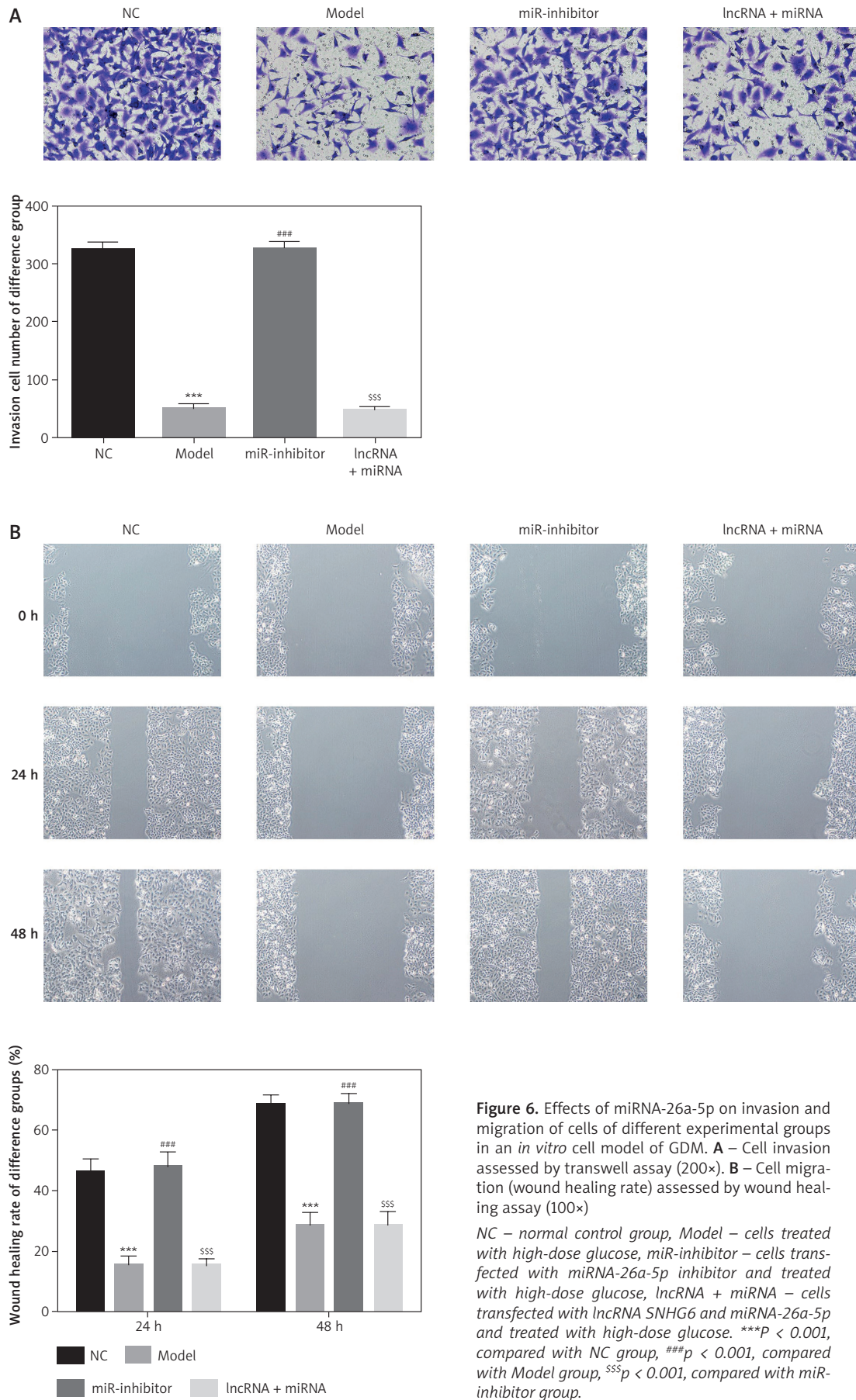


Figure 5. Cont. E – Apoptosis rate determined by flow cytometry
 NC – normal control group, Model – cells treated with high-dose glucose; miR-inhibitor: cells transfected with miRNA-26a-5p inhibitor and treated with high-dose glucose, lncRNA + miRNA: cells transfected with lncRNA SNHG6 and miRNA-26a-5p and treated with high-dose glucose. ****P* < 0.001, compared with NC group, ###*p* < 0.001, compared with Model group, SSS*p* < 0.001, compared with miR-inhibitor group.

these studies [20]. In our study, miR-26a-5p played an important role with lncRNA SNHG6 in improving the pathogenesis of GDM. Silencing miR-26a-5p could effectively alleviate the symptoms of GDM, whereas the positive role of SNHG6 disappeared after co-transfecting miR-26a-5p while overexpressing lncRNA SNHG6. This suggests that SNHG6 may improve the symptoms of GDM by inhibiting miR-26a-5p. Meanwhile, our study also demonstrated a significant increase in EZH2 protein and gene expression with overexpression of SNHG6 and suppressed expression of miR-26a-5p.

It was confirmed by dual-luciferase reporter gene assay that miR-26a-5p can target EZH2 in HTR-8/SVneo cells, and the abnormal expression of EZH2 may be related to the occurrence of GDM-induced placental villous cell function.

EZH2 is the catalytic core protein in polycomb repressive complex 2 (PRC2), which catalyzes and maintains trimethylation of histone H3 at lysine 27 (H3K27me3). This methylation site is an epigenetic marker related to gene silencing. A decrease in EZH2-H3K27me3 expression can inhibit cell proliferation and affect tumor progression in



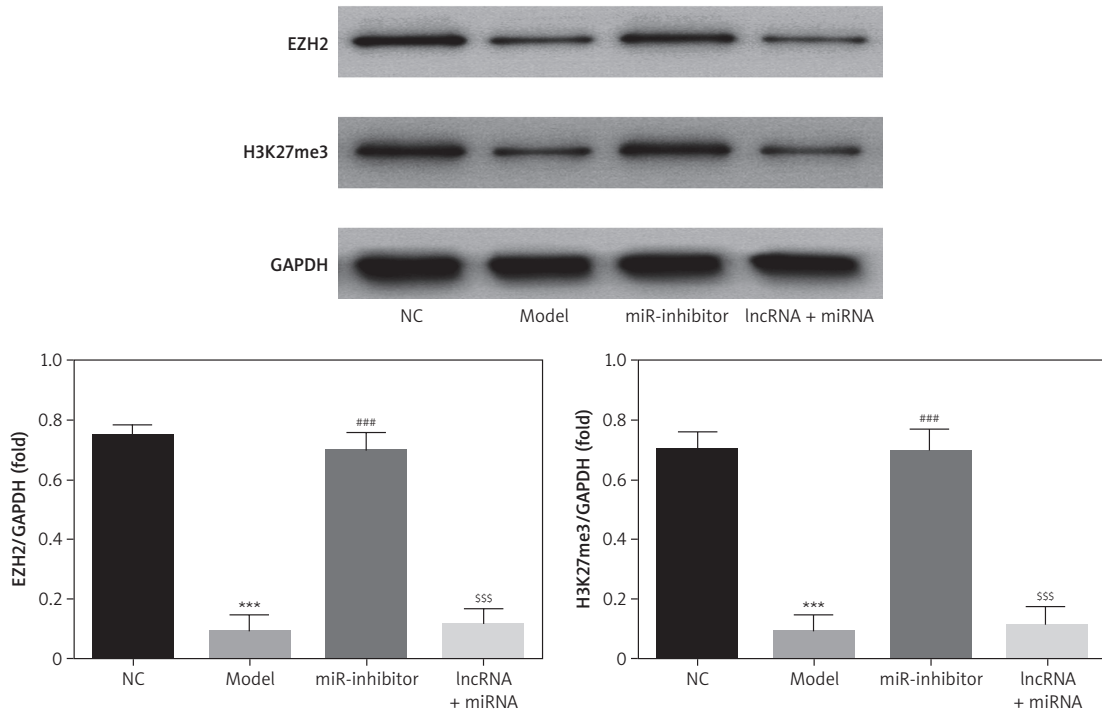


Figure 7. Effect of miRNA-26a-5p on relative expression of proteins as assessed by WB

NC – normal control group, Model – cells treated with high-dose glucose, miR-inhibitor – cells transfected with miRNA-26a-5p inhibitor and treated with high-dose glucose, lncRNA + miRNA – cells transfected with lncRNA SNHG6 and miRNA-26a-5p and treated with high-dose glucose. ****P* < 0.001, compared with NC group, ###*p* < 0.001, compared with Model group, SSS*p* < 0.001, compared with miR-inhibitor group.

Position 250-257 of EZH2 3'UTR	5' ...ACUUUGAAUAAAGAAUACUUGAA	8mer	-0.58	99	-0.58	4.646	0.85
hsa-miR-26-5p	3' UCGGAUAGGACCUAUGAACUU						

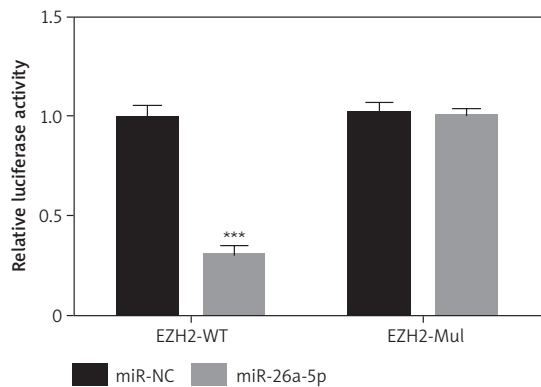


Figure 8. Correlation between miRNA-26a-5p and EZH2

****P* < 0.001, compared with miR-NC group.

lung cancer, bladder transitional cell carcinoma, and embryonal rhabdomyosarcoma. Inhibition of the EZH2-H3K27me3 pathway enhanced chemosensitivity to fluorouracil in hepatoma cells [21]. Siddiqi *et al.* [22] reported that regulation of the EZH2-H3K27me3 pathway could reduce expression of endogenous antioxidant inhibitor thioredoxin interaction protein (TXNIP), suppress the oxidative stress response, and alleviate proteinuria and other symptoms, so as to regulate the progress of diabetic nephropathy at the epigenetic level. In the

present study, there was decreased expression of SNHG6 and EZH2 in placental tissues from subjects with GDM. *In vitro* experiments showed that the expression of SNHG6 and miR-26a-5p was closely related to the expression of EZH2 and H3K27me3 in HTR-8/SVneo cells. Following upregulation of SNHG6 expression and inhibition of miR-26a-5p expression, the proliferation and infiltration abilities of the cells were significantly enhanced.

In conclusion, lncRNA SNHG6 can affect the function of trophoblasts, enhancing the prolifera-

tion, invasion, and migration ability of trophoblasts by regulating the miR-26a-5p/EZH2-H3K27me3 pathway. The findings of this study suggest that lncRNA SNHG6 may be an essential factor in the prevention of GDM and could facilitate the development of novel therapeutics for GDM to secure the outcome of future generations.

Conflict of interest

The authors declare no conflict of interest.

References

1. Hanson MA, Bardsley A, De-Regil LM, et al. The International Federation of Gynecology and Obstetrics (FIGO) Recommendations on adolescent, preconception, and maternal nutrition: "think nutrition first". *Int J Gynaecol Obstet* 2015; 131 Suppl 4: S213-53.
2. Abouzeid M, Versace VL, Janus ED, et al. Socio-cultural disparities in GDM burden differ by maternal age at first delivery. *PLoS One* 2015; 10: e0117085.
3. Assaf-Balut C, García de la Torre N, Durán A, et al. A Mediterranean diet with additional extra virgin olive oil and pistachios reduces the incidence of gestational diabetes mellitus (GDM): a randomized controlled trial: The St. Carlos GDM prevention study. *PLoS One* 2017; 12: e0185873.
4. Lu D, Yang M, Yao Y, Xie Y. A clinical research study on the respective relationships between visfatin and human fetuin A and pregnancy outcomes in gestational diabetes mellitus. *Taiwan J Obstet Gynecol* 2019; 58: 808-13.
5. Hepp P, Hutter S, Knabl J, et al. Histone H3 Lysine 9 acetylation is downregulated in gdm placentas and citriol supplementation enhanced this effect. *Int J Mol Sci* 2018; 19: E4061.
6. Moen GH, Sommer C, Prasad RB, et al. Epigenetic modifications and gestational diabetes: a systematic reviewer of published literature. *Eur J Endocrinol* 2017; 176: R247-67.
7. Szemraj-Rogucka ZM, Szemraj J, Masiarek K, Majos A. Circulating microRNAs as biomarkers for myocardial fibrosis in patients with left ventricular non-compaction cardiomyopathy. *Arch Med Sci* 2019; 15: 376-84.
8. Abdelsalam L, Ibrahim AA, Shalaby A, et al. Expression of miRNAs-122, -192 and -499 in end stage renal disease associated with acute myocardial infarction. *Arch Med Sci* 2019; 15: 1247-53.
9. Ding Y, Wang X, Pan J, et al. Aberrant expression of long non-coding RNAs (lncRNAs) is involved in brain glioma development. *Arch Med Sci* 2019; 16: 177-88.
10. Xu M, Chen X, Lin K, et al. lncRNA SNHG6 regulates EZH2 expression by sponging miR-26a/b and miR-214 in colorectal cancer. *J Hematol Oncol* 2019; 12: 3.
11. Li Y, Li D, Zhao M, et al. Long noncoding RNA SNHG6 regulates p21 expression via activation of the JNK pathway and regulation of EZH2 in gastric cancer cells. *Life Sci* 2018; 208: 295-304.
12. Zhang M, Duan W, Sun W. lncRNA SNHG6 promotes the migration, invasion, and epithelial-mesenchymal transition of colorectal cancer cells by miR-26a/EZH2 axis. *Onco Targets Ther* 2019; 12: 3349-60.
13. Ding GL, Wang FF, Shu J, et al. Transgenerational glucose intolerance with Igf2/H19 epigenetic alterations in mouse islet induced by intrauterine hyperglycemia. *Diabetes* 2012; 61: 1133-42.
14. Hamlett WC. Ultrastructure of the maternal-fetal interface of the yolk sac placenta in sharks. *Ital J Anat Embryol* 2005; 110 (2 Suppl 1): 175-81.
15. Zhang Y, Wu H, Wang F, Ye M, Zhu H, Bu S. Long non-coding RNA MALAT1 expression in patients with gestational diabetes mellitus. *Int J Gynaecol Obstet* 2018; 140: 164-9.
16. Shi Z, Zhao C, Long W, Ding H, Shen R. Microarray expression profile analysis of long non-coding RNAs in umbilical cord plasma reveals their potential role in gestational diabetes-induced macrosomia. *Cell Physiol Biochem* 2015; 36: 542-54.
17. Vienberg S, Geiger J, Madsen S, Dalgaard LT. MicroRNAs in metabolism. *Acta Physiol* 2017; 219: 346-61.
18. Deilius JA. MicroRNAs as regulators of metabolic disease: pathophysiologic significance and emerging role as biomarkers and therapeutics. *Int J Obes* 2016; 40: 88-101.
19. Zhu Y, Tian F, Li H, Zhou Y, Lu J, Ge Q. Profiling maternal plasma microRNA expression in early pregnancy to predict gestational diabetes mellitus. *Int J Gynaecol Obstet* 2015; 130: 49-53.
20. Aires MB, Dos Santos AC. Effects of maternal diabetes on trophoblast cells. *World J Diabetes* 2015; 6: 338-44.
21. Vella S, Pomella S, Leoncini PP, et al. MicroRNA-101 is repressed by EZH2 and its restoration inhibits tumorigenic features in embryonal rhabdomyosarcoma. *Clin Epigenetics* 2015; 7: 82.
22. Siddiqi FS, Majumder S, Thai K, et al. The histone methyltransferase enzyme enhancer of zeste homolog 2 protects against podocyte oxidative stress and renal injury in diabetes. *J Am Soc Nephrol* 2016; 27: 2021-34.